Accepted Manuscript

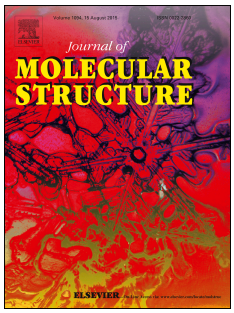

Crystallographic evidence for resonance assisted H-Bonding effect in selective colorimetric detection of cyanide by arylamino-naphthoquinones

P. Rajalakshmi, P. Jayasudha, Samuele Ciattini, Laura Chelazzi, Kuppanagounder P. Elango

PII: S0022-2860(19)30696-9

DOI: https://doi.org/10.1016/j.molstruc.2019.05.124

Reference: MOLSTR 26631

To appear in: *Journal of Molecular Structure*

Received Date: 14 February 2019

Revised Date: 9 May 2019

Accepted Date: 28 May 2019

Please cite this article as: P. Rajalakshmi, P. Jayasudha, S. Ciattini, L. Chelazzi, K.P. Elango, Crystallographic evidence for resonance assisted H-Bonding effect in selective colorimetric detection of cyanide by arylamino-naphthoquinones, *Journal of Molecular Structure* (2019), doi: https://doi.org/10.1016/j.molstruc.2019.05.124.

Crystallographic Evidence for Resonance Assisted H-Bonding Effect in Selective Colorimetric Detection of Cyanide by Arylamino-Naphthoquinones

P. Rajalakshmi, P. Jayasudha and Kuppanagounder P. Elango*

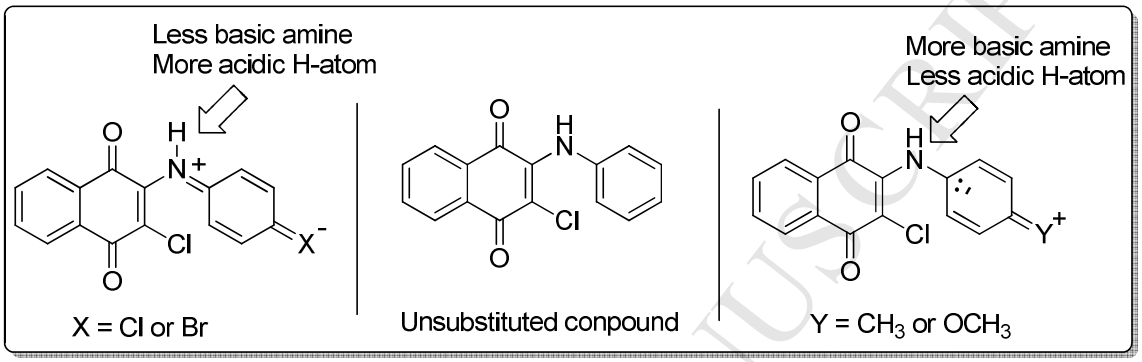

Crystallographic Evidence for Resonance Assisted H-Bonding Effect in Selective Colorimetric Detection of Cyanide by Arylamino-Naphthoquinones

P. Rajalakshmi[a], P. Jayasudha[a], Samuele Ciattini[b], Laura Chelazzi[b] and Kuppanagounder P. Elango[a]*

[a]Department of Chemistry, Gandhigram Rural Institute (Deemed to be University), Gandhigram 624302, India

[b]Centro di Cristallografia Strutturale, Università degli studi di Firenze, 50019, Sesto Fiorentino (Fi), Italy

Abstract

Five new chemo-receptors, based on arylamino-naphthoquinone, possessing electron donating and electron withdrawing substituents have been prepared by single step green method. These receptors are found to be highly selective and sensitive towards cyanide ions in aqueous HEPES buffer solution (pH 7.2). The mechanism, as evidenced by ^{1}H NMR, electrochemical and theoretical studies, is based on instantaneous deprotonation of –NH moiety by cyanide, which is enabled by substituent dependent resonance effect of the phenyl ring. This is confirmed by single crystal XRD data. The detection limit is calculated to be in the order of 10^{-8} M, which is much lower than the permissible limit of cyanide in drinking water set by WHO (1.9×10^{-6} M).

Keywords: Cyanide; Colorimetry; Quinone; Resonance; Sensing

---

* Corresponding author. Tel.: +91 451 245 2371; Fax: +91 451 2454466

E-mail: drkpelango@rediffmail.com (Prof. K.P. Elango)

1. Introduction

During recent past selective and sensitive methods to detect anions have received substantial attention due to the fundamental and important roles of anions in environmental, industrial and biological processes. Among the anions, cyanide ion sensing has attracted relatively more attention due to its high toxicity [1]. Water soluble cyanide salts are one of the most lethal chemicals and the permissible limit of cyanide in drinking water is 1.9 μM, according to World Health Organization (WHO) [2]. Review of literature revealed that the mechanism of interaction between cyanide ion and chemoreceptors include predominantly H-bonding [3-6], reaction-based sensors [7-14], electrostatic interaction [15-17] or metal-ligand interactions [18-20]. From the practical application view-point, a good receptor should not only be highly selective and sensitive but also easy to prepare and simple to operate. Thus, the developmental of new chemosensors for colorimetric detection of cyanide in aqueous solution is essential.

Recently we are in the process of developing quinone based chemosensors for selective colorimetric sensing of cyanide and fluoride ions in aqueous solution, that work via modulation of intramolecular charge transfer (ICT) transition. We have reiterated the selection of quinone as the signaling unit in all these reports. In continuation of our efforts to develop new chemo-receptors for colorimetric detection of anions in aqueous solution, here in this article we report the colorimetric sensing of cyanide by five arylamino-naphthoquinones (**R1**-**R5**) in aqueous solution. The anion sensing behaviour of these receptors has been investigated using spectral (UV-Vis, Fluorescence, ^{1}H NMR), electrochemical (Differential Pulse Voltammetry, DPV) and theoretical (DFT) studies.

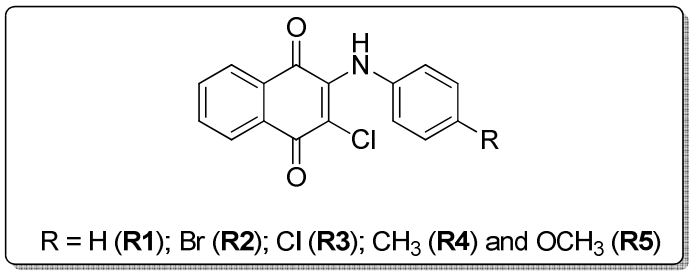

The selection of these chemo-receptors for the present study is due to the following reasons: i) we have reported an easy green protocol for the preparation of these molecules in solid state from commercially available starting materials, ii) the molecules themselves absorbs in the visible region and thus are coloured due to the existence of ICT transition from –NH moiety to electron deficient quinone ring, iii) further, any small perturbation in the electron density in the –NH receptor unit as a result of interaction with anion, would significantly alter the easiness of ICT transition and consequently would change the colour, and iv) furthermore, by changing the substituent R in the molecule, we can tune the acidity of the –NH proton and hence can very its intensity of interaction with the anion.

For comparison purpose, we have selected the following molecules **I-III** and studied their anion sensing behaviour also.

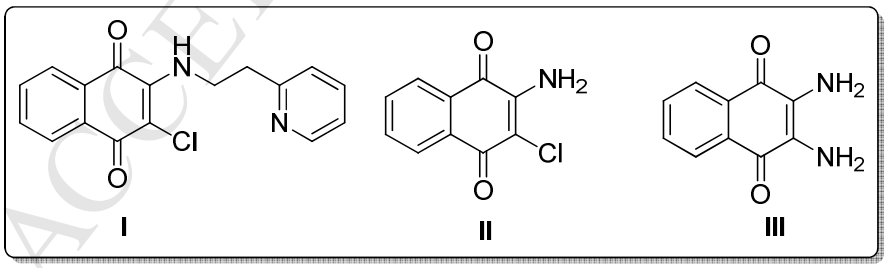

Interestingly, the chemo-receptors **R1-R5** selectively detect cyanide ion in aqueous solution with visible colour change, but not the other molecules (**I-III**). Based on the experimental results a

plausible resonance enabled mechanism for the sensing process has been proposed and discussed.

2. Experimental section

2.1 Chemicals and apparatus. All the reagents for the preparation of the receptors were obtained commercially and were used without further purification. Spectroscopic grade solvents were used as received. Doubly distilled water was used throughout the work and the second distillation was carried out using alkaline permanganate. UV-Vis spectral studies were carried out on a double beam spectrophotometer. Steady state fluorescence spectra were obtained on a spectrofluorimeter. The excitation and emission slit width (5 nm) and the scan rate (250 mVs^{-1}) was kept constant for all of the experiments. Nuclear magnetic resonance spectra were recorded in DMSO-d_6 (400 MHz). The ^{1}H NMR spectral data is expressed in the form: Chemical shift in units of ppm (normalized integration, multiplicity, and the value of J in Hz). The differential pulse voltammetry (DPV) experiments, of 1 mmol solutions of the compounds, were carried out using GC as working, Pt wire as reference and Ag wire as auxiliary electrodes in dimethylformamide containing 0.1 M tetrabutylammonium perchlorate as supporting electrolyte at a scan rate of 100 mVs^{-1}.

2.2 Preparation and characterization of receptors. The receptors were prepared as reported, by us earlier, from commercially available 2,3-dichloro-1,4-naphthoquinone and *para*-substituted anilines via solid state reaction [21]. The overall reaction is given in Scheme 1.

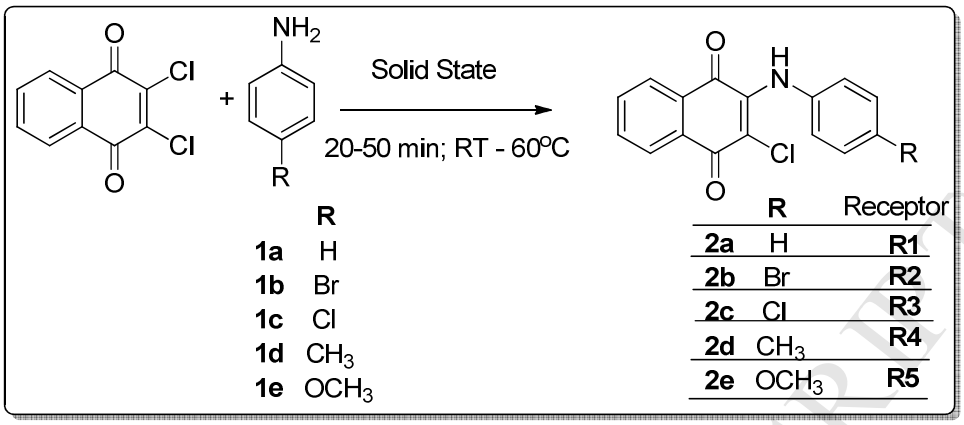

Scheme 1. Preparation of receptors (**R1-R5**)

The receptors were characterized using ^{1}H NMR and HRMS-ESI spectral techniques. The results matched well with those reported earlier [21]. Receptor **R1**: Red solid (yield 85%); Melting Point: 220^{o}C; ^{1}H (400 MHz; DMSO-d_6; Me_4Si/ppm): 7.13-7.15 (m, 3H), 7.30-7.34 (t, *J*=8 Hz, 8 Hz, 2H), 7.79-7.89 (m, 2H), 8.03-8.05 (d, *J*=8Hz, 2H), 9.32 (s, 1H) (Fig. S1); ^{13}C NMR (100 MHz, DMSO-d_6) δ 114.71,124.43, 124.85, 126.55, 127.00, 128.39, 130.74, 132.43, 133.66, 135.26, 139.30, 143.62, 177.16, 180.59 (Fig. S2); LCMS (ESI-APCI) m/z: Calculated for $C_{16}H_{10}ClNO_2$ $[M+H]^+$ 283.7 found 284.1 (Fig. S3); FT-IR (KBr), cm^{-1}: 3245 (N-H), 1675, 1637 (C=O), 1331 (C-N) (Fig. S4); Receptor **R2**: Red solid (yield 85%); Melting Point: 240^{o}C; ^{1}H (400 MHz; DMSO-d_6; Me_4Si/ppm): 7.08-7.10 (d, *J*=8 Hz, 2H), 7.48-7.50 (d, *J*=8 Hz, 2H), 7.80-7.90 (m, 2H), 8.04-8.06 (m, 2H) 9.35 (s, 1H) (Fig. S5); ^{13}C NMR (100 MHz, DMSO-d_6) δ 120.59, 121.45, 130.79, 131.33, 131.76, 135.55, 135.93, 137. 09, 138.52, 139.99, 143.62, 148.20, 182.01, 185. 23 (Fig. S6); LC-MS (ESI-APCI) m/z: Calculated for $C_{16}H_9BrClNO_2$ $[M+H]^+$ 362.61 found 364. 1 (Fig. S7); FT-IR (KBr), cm^{-1}: 3242 (N-H), 1675, 1638 (C=O), 1329 (C-N) (Fig. S8); Receptor **R3**: Red solid (yield 81%); Melting Point: 260^{o}C; ^{1}H (400 MHz; DMSO-d_6; Me_4Si/ppm): 7.13-7.15 (d, *J*=8 Hz, 2H), 7.35-7.38 (d, *J*=12 Hz, 2H), 7.80-7.89 (m, 2H), 8.03-

8.05 (d, *J*=8 Hz, 2H), 9.37 (s, 1H) (Fig. S9); ^{13}C NMR (400 MHz, DMSO-d_6) δ 115.65, 125.75, 126.58, 127.01, 128.28, 128.60, 130.80, 132.36, 133.75, 135.24, 138.44, 143.53, 177.25, 180.48 (Fig. S10); LC-MS (ESI-APCI) m/z: Calculated for $C_{16}H_9Cl_2NO_2$ $[M+H]^+$ 318.15 found 318.1 (Fig. S11); FT-IR (KBr), cm^{-1}: 3234 (N-H), 1675, 1639 (C=O), 1329 (C-N) (Fig. S12); Receptor **R4**: Red solid (yield 83%); Melting Point: 202^{o}C; ^{1}H (400 MHz; DMSO-d_6; Me_4Si/ppm): 2.30 (s, 3H), 7.02-7.04(d, *J*=8 Hz, 2H), 7.11-7.14 (d, *J*=12 Hz, 2H), 7.80-7.89 (m, 2H), 8.03-8.04 (d, *J*= 4 Hz, 2H), 9.26 (s, 1H) (Fig. S13); ^{13}C NMR (400 MHz, DMSO-d_6) δ 21.03,113.79, 124.61, 126.52, 126.97, 128.86, 130.66, 132.49, 133.56, 134.20, 135.27, 136.65, 143.65, 177.03, 180.62 (Fig. S14); LC-MS (ESI-APCI) m/z: Calculated for $C_{17}H_{12}ClNO_2$ $[M+H]^+$ 297.74 found 298.1 (Fig. S15); FT-IR (KBr), cm^{-1}: 3226 (N-H), 1676, 1635 (C=O), 1329 (C-N) (Fig. S16); Receptor **R5**: Red solid (yield 87%); Melting Point: 198^{o}C; ^{1}H (400 MHz; DMSO-d_6; Me_4Si/ppm): 2.30 (s, 3H), 7.02-7.04 (d, *J*=8 Hz, 2H), 7.12-7.14 (d, *J*=8 Hz, 2H), 7.81-7.89 (m, 2H), 8.03-8.04 (d, *J*= 4 Hz, 2H), 9.26 (s, 1H) (Fig. S17); ^{13}C NMR (400 MHz, DMSO-d_6) δ 21.04, 113.79, 124.61, 126.53, 126.98,128.87, 130.67, 132.50, 133.58, 134.21, 135.28, 136.66, 143.67, 177.05, 180.63 (Fig. S18); LC-MS (ESI-APCI) m/z: Calculated for $C_{17}H_{12}ClNO_3$ $[M+H]^+$ 313.74 found 314.2 (Fig. S19); FT-IR (KBr), cm^{-1}: 3228 (N-H); 1675, 1639 (C=O), 1329 (C-N) (Fig. S20).

The compound **I** is reported by us [22], **II** is commercially available and **III** is prepared by adopting the reported procedure [23].

3. Results and discussion

Five new arylamino-naphthoquinone derivatives (**R1-R5**) were prepared and characterized using NMR and mass spectral techniques. The anion sensing behaviour of these

chemo-receptors has been investigated using various spectral, electrochemical and theoretical studies. Based on the results a plausible mechanism has been proposed and discussed.

3.1 Visual detection experiment. As a preliminary screening the change in colour of the receptors in the absence and presence of one equivalent of various anions has been observed in aqueous HEPES buffer:DMF (2:8 v/v) solution. As seen from Figures 1 and S21, the colour of the receptor solutions changed instantaneously from red-orange to blue with the addition of cyanide ion. However, addition of other chosen anions didn't produce any colour change indicating high selectivity of these receptors towards cyanide ion. Likewise, the change in colour of the solution of **R1**, as a representative case, upon addition of cyanide ion at different pH values was also observed (Fig. S22). The receptor **R1** was found to produce similar colour change in 7-11 pH range. Surprisingly the compounds **I-III** were not able to produce any colour change with these anions, including cyanide ion in aqueous HEPES buffer:DMF (2:8 v/v) solution (pH 7.2).

3.2 UV-Vis spectral studies. With an aim to confirm the selectivity of these receptors towards cyanide ion, the UV-Vis spectra of **R1** were recorded, in aqueous HEPES buffer:DMF (2:8 v/v) solution, with addition of one equivalent of various anions and the spectra obtained is depicted in Figure 2. As evidenced from the spectra, addition of cyanide ion red-shifted the absorption maximum of **R1** from 481 nm to 589 nm ($\Delta\lambda$ 109 nm). While all the other anions caused no observable change in the spectrum of **R1**, confirming high selectivity of the receptor towards cyanide ion. The UV-Vis spectra of these receptors with addition of incremental amounts of cyanide ions were also recorded aqueous HEPES buffer:DMF (2:8 v/v) solution (Fig. 3 and S23-26). In all these cases, upon addition of incremental amounts of cyanide ions, the absorption maximum around 480 nm decreased with a concomitant increase in absorption maximum of a

new peak around 590 nm with a single isosbestic point (Table 1). The appearance of single isosbestic point indicated the presence of only two species in equilibrium [24]. Further, the high magnitude of the molar extinction coefficient values of the new peak made the visual detection of cyanide ion easy (Table 1).

3.3 Fluorescence spectral studies. The binding constants for the interaction of these receptors with cyanide ion were determined using fluorescence spectral titration data. The fluorescence spectra of **R1**-**R5** with incremental addition of cyanide in aqueous HEPES buffer:DMF (2:8 v/v) solution have been recorded and the spectra obtained are given in Figures 4 and S27-30. It is evident from the spectra that addition of incremental amounts of cyanide was found to significantly quench the fluorescence of these receptors, suggesting strong interaction between them. From the fluorescence quenching data the binding constants for the interaction between the receptors and cyanide were calculated using the following equation [25, 26].

$$\log (F_0\text{-}F)/F = \log K_A + n \log [Q]$$

Where F_0 is the emission intensity in the absence of quencher [Q], F is the emission intensity at the quencher concentration [Q] and K_A is the binding constant for the receptor-CN^- ion complex. In all the cases, a plot of log (F_0-F) versus log [Q] was found to be linear ($r > 0.99$) and the binding constants calculated are also collected in Table 1. The order of binding constant values was observed to be: **R2** (Br) > **R3** (Cl) > **R1** (H) > **R4** (CH_3) > **R5** (OCH_3). The observed order indicated that the receptors with electron withdrawing substituents bind strongly with cyanide than the unsubstituted compound, while those with electron donating substituents bind relatively weakly with cyanide ion. The stoichiometry of the binding between these receptors and cyanide was determined using fluorescence data and the Job's plot obtained is shown in Figure S31 [27].

In the Job's plots of all these cases curves with a maximum at mole fraction 0.5 suggested a 1:1 stoichiometry between the receptors and cyanide ion. The fluorescence spectral data were used to calculate the detection limit of these receptors as described elsewhere [28-30]. The results collected in Table 1 indicated that the detection limit was observed to be in the order of 10^{-8} M, which is lower than the maximum level of cyanide in drinking water that the WHO permits ($1.9x10^{-6}$ M).

3.4 ^{1}H NMR spectral studies. In order to delineated the mechanism of detection of cyanide by these receptors, ^{1}H NMR titration studies were carried out in DMSO-d_6. As a representative case the ^{1}H NMR spectra of **R1** with addition of 0-1 equivalent of cyanide were shown in Figure 5 and the spectra of other receptors are collected in Figures S32-41. The ^{1}H NMR spectrum of free **R1** exhibited a signal at δ 9.32 ppm corresponding to –NH proton. In the absence of cyanide ion, the aromatic protons appeared at δ 7.13-8.05 ppm. As shown in Figure 5, upon addition of incremental amounts of cyanide, the signal at 9.32 ppm decreased gradually and showed upfield shift and after adding one equivalent of cyanide this signal disappeared completely suggesting deprotonation of –NH moiety by the added cyanide ion. The signal for the –NH proton in free **R1** appeared at 9.32 ppm, which is higher than that of free aniline in DMSO-d_6 (δ 4.99 ppm). This may be due to the existence of ICT transition from –NH moiety to the electron deficient quinone ring. However, if ICT transition is the only contributing factor for the enhanced acidity of the –NH proton, compounds **I** and **II** should also exhibited nearly similar signal for the –NH protons. But, it is not so. Therefore, in the case of **R1** resonance effect of the phenyl ring might also contributed significantly to the acidity of the proton. This presumption is further supported by the fact that the chemical shift of the –NH proton in the receptors under investigation (**R1**-**R5**) was found to be substituent dependent. The receptors with electron withdrawing substituents

showed δ_{NH} greater than 9.32 ppm, while that with electron donating substituents had chemical shifts less than 9.32 ppm for the –NH proton. It is also evident from Figures 5 and S32-41 that upon addition of one equivalent of cyanide, the proton peak of phenyl ring showed substantial upfield shift. This may be due to the fact that the electron density generated on N-atom might have been distributed in the phenyl ring through resonance [31]. It is noteworthy to understand that the compounds **I-III** failed to detect cyanide under the experimental conditions, even if present in large excess. They showed no colour and spectral changes upon addition of cyanide ion in aqueous HEPES buffer:DMF (2:8 v/v) solution. Based on these findings, we propose a deprotonation mechanism for the detection of cyanide by these receptors and this is enabled by resonance effect.

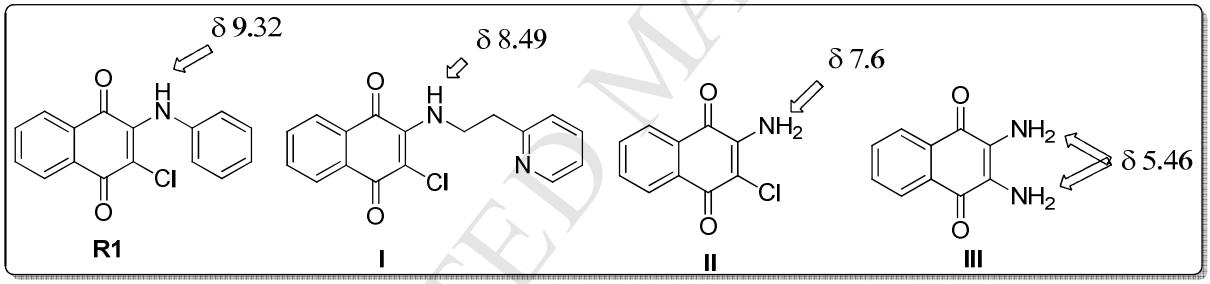

It is well established that resonance effect greatly influences the basicity of aniline (and consequently the acidity of the –NH proton). Electron withdrawing substituents through resonance effect would increase the acidity of the –NH proton when compared to the unsubstituted compound, while electron donating substituents would exhibit opposite effect.

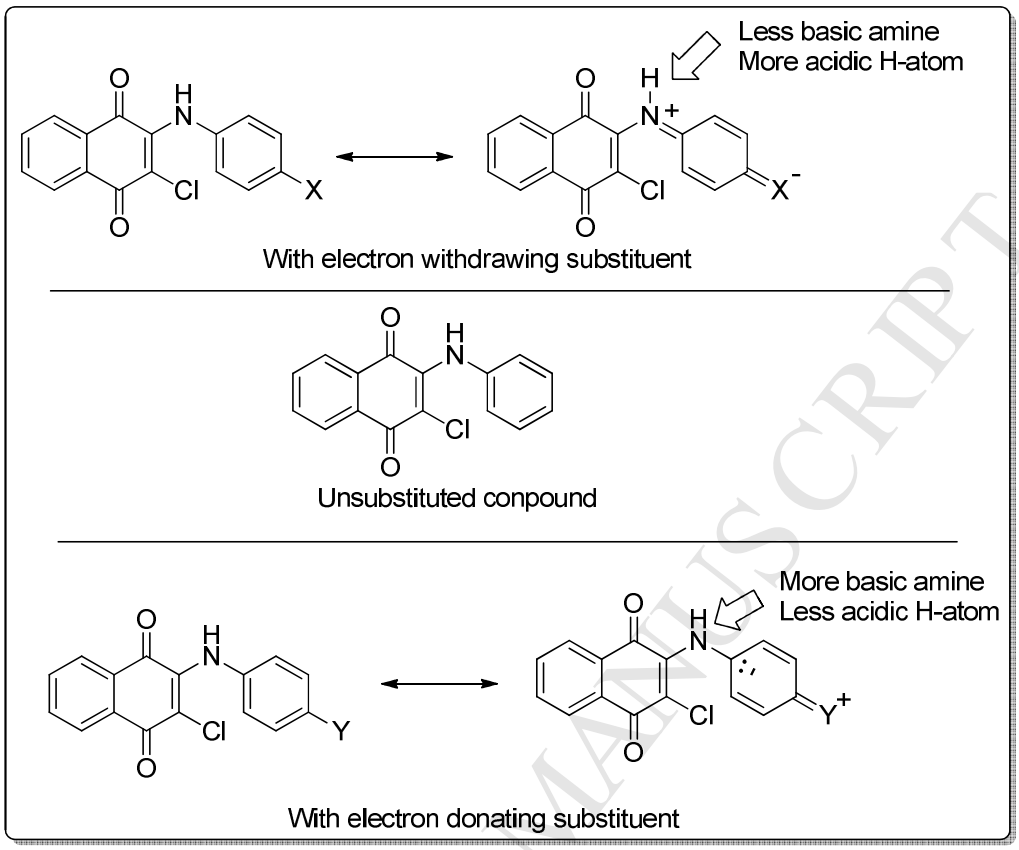

Hence, it would be relatively easy to deprotonate the –NH proton from receptors possessing electron withdrawing substituents when compared to the unsubstituted compound. In other words, the electron density generated on N-atom, upon deprotonation by cyanide ion, would be stabilized by electron with drawing substituents through resonance. Consequently such receptors would exhibit relatively higher binding constants than that of the unsubstituted one. While those with electron donating substituents would show relatively lower binding constant values than the unsubstituted compound. This is in line with the order of binding constants observed in fluorescence spectral studies. Hence, it may be concluded that resonance effect plays a significant role in deciding the easiness of deprotonation of the –NH proton by the added cyanide ion.

3.5 Single crystal XRD study. The molecular structures of **R3** and **R4** were confirmed by single crystal XRD study. The structures with atom numbering are given in Figure 6 and the crystal data are collected in Table T1. The bond lengths and bond angles are given in Tables T2-T5. Bertolasi et al. [32] have discussed the strength of intermolecular H-bonds of N-H moiety in heteroconjugated systems (including receptor **R1**) using single crystal XRD data. In these enaminonic O=C−C=C−NHR groups C=O distances have been chosen as the indicators of π-delocalization within the fragment. They concluded that there is a direct relationship between the strength of the H-bond and lengthening of the C=O bond distance. The selected bond lengths in **R1**, **R3** and **R4** are depicted below.

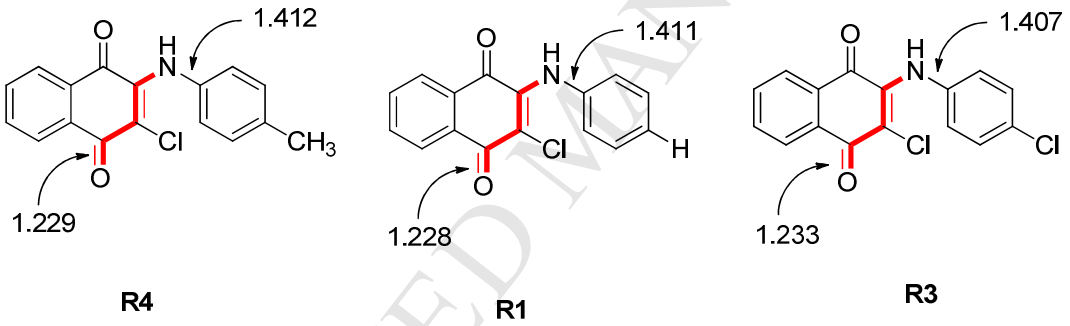

R4 **R1** **R3**

The bond lengths for **R1** were taken from Ref. [32]. It is evident from the data that in receptor with chloro-substituent (**R3**) the relatively longer C(11)=O(2) bond distance (1.233 Å), when compared to the unsubstituted compound, is indicative of stronger H-bonding ability of the N−H moiety. This is possible due to the resonance assisted H-bonding i.e. the charge density on the N(1)-atom is removed through resonance by the C(11)=O(2) group. It is also evident that the charge density on the N-atom is also reduced by the resonance effect of the chloro-substituent leading to relatively shorter N(1)−C(4) distance (1.407 Å). Such resonance assisted removal of the charge density from the N(1)-atom would make the H-atom (of N−H) more acidic and could interact with cyanide ions strongly, as seen above. Thus, the bond distance data strongly

supported the proposed role resonance effect on the cyanide sensing behaviour of these receptors.

3.6 Electrochemical study. The foregoing ^{1}H NMR spectral studies suggested that the resonance effect dominates over ICT transition influence on the cyanide detection mechanism. In order to substantiate the ^{1}H NMR spectral studies, electrochemical behaviour of these receptors in the absence and presence of increasing concentration of cyanide has been investigated. The DP voltammograms of these receptors recorded in DMF are depicted in Figures 7 and S42-45. It is evident from the figures that, all the receptors showed a typical voltammogram for the electro-reduction of the quinone ring with two reduction peaks (at E_{pc} = **R1**: -0.6207, -0.9981; **R2**: -0.6267, -0.9744; **R3**: -0.6440, -1.0079; **R4**: -0.5654, -1.0730 and **R5**: -0.6188, -1.0098 V). It is well established that in the case of quinones the first reduction peak at a lower negative potential corresponds to the formation of radical anion ($Q^{\bullet-}$) and the second reduction peak at a relatively higher negative potential corresponds to the formation of dianion (Q^{2-}) [33]. The electro-reduction of 2,3-dichloro-1,4-naphthoquinone, under similar experimental conditions in DMF, showed two reduction peaks at -0.3103 and -1.1320 V [34]. From these values it evident that the electro-reduction of the quinone ring in **R1** (substituted with arylamine) is relatively difficult when compared to that of 2,3-dichloro-1,4-naphthoquinone (containing two electron withdrawing Cl-atoms), suggesting existence of ICT transition in **R1**. As shown in the voltammograms, with addition of incremental amounts of cyanide to the solution of these receptors, both the reduction peaks are shifted to lesser negative potential with a concurrent decrease in current density. That is upon addition of cyanide the electro-reduction of the quinone becomes relatively easier [35]. If the negative charge generated on N-atom, upon deprotonation of –NH moiety, dissipates into the quinone ring, the electro-reduction would have become

increasingly difficult [24]. But in the present study, electro-reduction of the quinone ring becomes increasingly easier with an increase in concentration of cyanide ion. This observation suggested that the negative charge generated on N-atom is stabilized by resonance effect of the phenyl ring, which is in line with the observations made in ^{1}H NMR spectral studies.

3.7 Theoretical study. DFT computations were used to further understand the cyanide detection process by the receptors under investigation. The calculations were performed at B3LYP/6-311G level basis set using Gaussian 03 package [36]. The frontier molecular orbitals (HOMO and LUMO) generated for **R** and **R**+$\mathbf{CN}^{-}$ species are shown in Figures 8 and S46-49. As seen from the figures, in free receptors HOMO is concentrated on the arylamino moiety and LUMO is localized on the quinone moiety as expected. Such a distribution of MO's is prerequisite for a compound to be a good ICT probe [37]. This confirms that the electronic transition (ICT) occurs from arylamino moiety to quinone ring. Further, decrease in energy gap between HOMO and LUMO from **R** to **R**+$\mathbf{CN}^{-}$ is responsible for the red-shift observed in the UV-Vis spectra of the receptor upon addition of cyanide ion. The electron distribution in **R**+$\mathbf{CN}^{-}$ is quite different from that of **R** both in HOMO and LUMO. Both these MO's have almost identical charge distribution in **R**+$\mathbf{CN}^{-}$ species, suggesting that the transition is assigned to the $\pi \rightarrow \pi^{*}$ transition of the depropotated arylamino moiety. Therefore, a charge separation cannot be expected to be generated while an electron is promoted from HOMO to LUMO in **R**+$\mathbf{CN}^{-}$. Thus, the ICT process is less obvious in **R**+$\mathbf{CN}^{-}$ than that in free **R**, which may be due to the significant resonance contribution of the phenyl ring to stabilize the charge generated upon deprotonation [38].

3.8 Practical application. The practical applicability of these receptors has been explored by means of preparing easy to use paper test strips. These strips were prepared by immersing filter

paper into an aqueous solution of **R1** (as a representative case) and drying in air (Fig. 9). The cyanide solutions of various concentrations were prepared in naturally occurring deep well water by dissolving required quantity of sodium cyanide. The composition of the water samples used in the present study is: (all in mg/L except pH) pH 7.98; Total alkalinity 403; Total hardness 244; Total dissolved solids 1416; Cl^- 197; F^- 1.02; SO_4^{2-} 36. As seen from the figure, when the test strips were immersed in aqueous solutions of cyanide, the colour of the strips immediately changed, which can be seen visually. Therefore, these paper strips can effectively been used as a test-kit for the detection of cyanide ion in natural water.

4. Conclusion

Chemo-receptors based on arylamino-naphthoquinone for colorimetric detection of cyanide have been developed and reported in this article. These receptors showed excellent colour change selectively and sensitively in aqueous solution via deprotonation mechanism as evidenced from ^{1}H NMR titration studies. The deprotonated N-atom was found to be stabilized by resonance effect of the phenyl ring. Also, the binding of cyanide with these receptors and resonance contribution was found to depend on the nature of the substituent attached to the phenyl ring in the *para*-position. Electrochemical and DFT studies supported the proposed mechanism.

Appendix A

CCDC numbers 1892810 and 1892811contain the supplementary crystallographic data for the receptor R3 and R4, respectively, given as CIF files. Crystallographic data can be obtained free of charge via http://www.ccdc.cam.ac.uk/conts/retrieving.html, or from the Cambridge Crystallographic Data Centre, 12 Union Road, Cambridge CB2 1EZ, UK; fax: (+44) 1223 336 033; or e-mail: deposit@ccdc.cam.ac.uk.

Reference

[1] C. Arivazhagan, B. Rosmita, R. Jagan, S. Ghosh, Benzoindolium-Triarylborane Conjugates: Ratiometric Fluorescent Chemodosimeter for the Detection of Cyanide ions in Aqueous Medium, Dalton Trans. 45 (2016) 5014-5020.

[2] Guidelines for Drinking-Water Quality, World Health Organization, Genova, 12 (2011) 342–344.

[3] P. Anzenbacher, D.S. Tyson, K. Jursikova, F.N. Castellano, Luminescence Lifetime-Based Sensor for Cyanide and Related Anions, J. Am. Chem. Soc. 124 (2002) 6232- 6233.

[4] S.H. Kim, S.J. Hong, J. Yoo, S.K. Kim, J.L. Sessler, C.H. Lee, Strapped Calix [4] pyrroles Bearing a 1,3-Indanedione at a β-Pyrrolic Position: Chemodosimeters for the Cyanide Anion, Org. Lett. 11 (2009) 3626-3629.

[5] N. Kumari, S. Jha, S. Bhattacharya, Colorimetric Probes Based on Anthraimidazolediones for Selective Sensing of Fluoride and Cyanide ion via Intramolecular Charge Transfer, J. Org. Chem. 76 (2011) 8215- 8222.

[6] M.Gemilli, Y.Nural, E.Keles, B.Aydiner, N.Seferoglu, E.Sahin, H.Sari, Z.Seferoglu, Novel 1,4-napthoquinone N-arylthioureas: syntheses, crystal structure, anion recognition properties, DFT studies and determination of acid dissociation constants, J. Mol. Struc. 269 (2018) 920-932.

[7] S. Wang, Y. Sie, C.Wan, A.Wu, A reaction-based fluorescent sensor for detection of cyanide in aqueous media, J. Lumin. 173 (2016) 25-29.

[8] S. Wang, X. Fei, J. Guo, Q. Yang, Y. Li, Y. Song, A novel reaction-based colorimetric and ratiometric fluorescent sensor for cyanide anion with a large emission shift and high selectivity, Talanta 148 (2016) 229-236.

[9] J.J. Lee, S.Y. Lee, K.H. Bok, C. Kim, A new Dual-Channel Chemosensor Based on Chemodosimeter Approach for Detecting Cyanide in Aqueous Solution: a Combination of Experimental and Theoretical Studies, J. Fluoresc. 25 (2015) 1449–1459.

[10] J.J. Li, W. Wei, X. L. Qi, X. Xu, Y.C. Liu, Q.H. Lin, W. Dong, Rational design, synthesis of reaction-based dual-channel cyanide sensor in aqueous solution, Spectrochim. Acta, Part A 152 (2016) 288-293.

[11] M.E. Jun, B. Roy, K.H. Ahn, Turn-on fluorescent sensing with reactive probes, Chem. Commun**.** 47 **(**2011) 7583-7601.

[12] J.F.Chen, Q.Lin, Y.M.Zhang, H.Yao, T.B.Wei, Pillararene-based fluorescent chemosensors: recent advances and perspectives, Chem. Commun.53 (2017) 13296-13311.

[13] Q.Lin, K.P.Zhong, J.H.Zhu, L.Ding, J.X.Su, H.Yao, T.B.Wei, Y.M.Zhang, Iodine controlled pillar[5]arene-based mutiresponsive supramolecular polymer for fluorescence detection of cyanide, mercury and cysteine, Macromolecules 50 (2017) 7863-7871.

[14] Q.Lin, T.T.Lu, X.Zhu, T.B.Wei, H.Li, Y.M.Zhang, Rationally introduce muti-competitive binding interactions in supramolecular gels: a simple and efficient approach to develop muti-analyte sensor array, Chem. Sci. 7 (2016) 5341-5346.

[15] M.R. Ajayakumar, P. Mukhopadhyay, Single-Electron Transfer Driven Cyanide Sensing: A New Multimodal Approach, Org. Lett. 12 (2010) 2646–2649.

[16] Z. Xu, X. Chen, H.N. Kim, J. Yoon, Sensors for the optical detection of cyanide ion, Chem. Soc. Rev. 39 (2010) 127-137.

[17] F. Wang, L. Wang, X. Chen, J. Yoon, Recent progress in the development of fluorometric and colorimetric chemosensors for detection of cyanide ions, Chem. Soc. Rev. 43 **(**2014) 4312-4324.

[18] P. Santanu, A.P. Chattopadhyay, K. Ghosh, Naphthalene and pyrrole substituted guanidine in selective sensing of Cu^{2+}, Hg^{2+}, Pb^{2+} and CN^{-} ions under different conditions, J. Supramol. Chem. 29 (2017) 528-535.

[19] C. Gomathy, Y. Chen, A.J. Karttunen, M.T. Dau, J. Jänis, S.P. Tunik, P. Chou, M. Ho, I. O. Koshevoy, Luminescent Triphosphine Cyanide d^{10} Metal Complexes, Inorg. Chem. 55 (2016) 2174–2184.

[20] T. Sun, Y. Li, Q. Niu, T. Li, Y. Liu, Highly selective and sensitive determination of Cu^{2+} in drink and water samples based on a 1,8-diaminonaphthalene derived fluorescent sensor, Spectrochim. Acta, Part A 195 (2018) 142-147.

[21] A. Satheshkumar, K.P. Elango, Spectroscopic and theoretical studies on the nucleophilic substitution of 2,3-dichloronaphthoquinone with para-substituted anilines in solid state via initial charge transfer complexation, Spectrochim. Acta, Part A 98 (2012) 378–383.

[22] A. Kosiha, C. Parthiban, K.P. Elango, Synthesis, characterization and DNA binding/cleavage, protein binding and cytotoxicity studies of Co(II), Ni(II), Cu(II) and Zn(II) complexes of aminonaphthoquinone, J. Photochem. Photobio. B 168 (2017) 165-174.

[23] R. Manivannan, A. Satheshkumar, E.H. El-Mossalamy, L.M. Al-Harbi, S.A. Kosa, K.P. Elango, Design, synthesis and characterization of indole based anion sensing receptors, New J. Chem. 39 (2015) 3936-3947.

[24] R. Manivannan, A. Satheshkumar, K.P. Elango, Tuning of the H-bonding ability of imidazole N–H towards the colorimetric sensing of fluoride and cyanide ions as their sodium salts in water, New J. Chem. 37 (2013) 3125-3160.

[25] A. Satheshkumar, K.P. Elango, Spectral and DFT studies on simple and selective colorimetric sensing of fluoride ions via enhanced charge transfer using a novel signaling unit, Dyes Pigm. 96 (2013) 364–371.

[26] F. Ding, G. Zhao, J. Huang, S. Ying, Z. Li, Fluorescence spectroscopic investigation of the interaction between chloramphenicol and lysozyme, J. Med. Chem. 44 (2009) 4083–4089.

[27] K.K. Upadhyay, R.K. Mishra, V. Kumar, P.K. Roy Chowdhury, A coumarin based ICT probe for fluoride in aqueous medium with its real application, Talanta 82 (2010) 312–318.

[28] S. Park, K.H. Hong, J.I. Hong, H.J. Kim, Azo dye-based latent colorimetric chemodosimeter for the selective detection of cyanides in aqueous buffer, Sens. Actuators, B 174 (2012) 140-144.

[29] Y. Yan, H. Yu, K. Zhang, M. Sun, Y. Zhang, X. Wang, S. Wang, Dual-emissive nanohybrid of carbon dots and gold nanoclusters for sensitive determination of mercuric ions, Nano Res. 9 (2016) 2088- 2096.

[30] Y. Zhang, L. Guan, H. Yu, Y. Yan, L. Du, Y. Liu, M. Sun, D. Huang, S. Wang, Reversible Fluorescent Probe for Selective Detection and Cell Imaging of Oxidative Stress Indicator Bisulfite, Anal. Chem. 88 (2016) 4426- 4431.

[31] Y. Yu, T. Shu, C. Dong, A convenient colorimetric and ratiometric fluorescent probe for detection of cyanide based on BODIPY derivative in aqueous media, Anal. Chem. 12 (2017) 34-39.

[32] V. Bertolasi, P. Gilli, V. Ferretti, G. Gilli, Intermolecular N-H…O hydrogen bonds assisted by resonance. Heteroconjugated systems as hydrogen bond strengthening functional groups, Acta Cryst., B51 (1995) 1004-1015.

[33] V.A. Nikitina, R.R. Nazmutdinov, G.A. Tsirlina, Quinones Electrochemistry in Room-Temperature Ionic Liquids, J. Phys. Chem. B 115 (2011) 668- 677.

[34] C. Ibis, S.S. Ayla, H. Asar, Synthesis and spectral and electrochemical characterization of novel substituted 1,4-naphthoquinone derivatives, Synth. Commun. 44 (2014)121–126.

[35] R. Manivannan, K.P. Elango, Structure–reactivity correlation in selective colorimetric detection of cyanide in solid, organic and aqueous phases using quinone based chemodosimeters, New J. Chem. 40 (2016)1554-1563.

[36] M.J. Frisch, G.W. Trucks, H.B. Schlegel, G.E. Scuseria, M.A. Robb, J.R.Cheeseman, J.A. Montgomery Jr., T. Vreven, K.N. Kudin, J.C. Burant, J.M. Millam, S.S. Iyengar, J. Tomasi, V. Barone, B. Mennucci, M. Cossi, G. Scalmani, N. Rega, G.A. Petersson, H. Nakatsuji, M. Hada, M. Ehara, K. Toyota, R. Fukuda, J. Hasegawa, M. Ishida, T. Nakajima, Y. Honda, O. Kitao, H. Nakai, M. Klene, X. Li, J.E. Knox, H.P. Hratchian, J.B. Cross, V. Bakken, C. Adamo, J. Jaramillo, R. Gomperts, R.E. Stratmann, O. Yazyev, A.J. Austin, R. Cammi, C. Pomelli, J.W. Ochterski, P.Y. Ayala, K. Morokuma, G.A. Voth, P. Salvador, J.J. Dannenberg, V.G. Zakrzewski, S. Dapprich, A.D. Daniels, M.C. Strain,

O. Farkas, D.K. Malick, A.D. Rabuck, K. Raghavachari, J.B. Foresman, J.V. Ortiz, Q. Cui, A.G. Baboul, S. Clifford, J. Cioslowski, B.B. Stefanov, G. Liu, A. Liashenko, P. Piskorz, I. Komaromi, R.L. Martin, D.J. Fox, T. Keith, M.A. Al-Laham, C.Y. Peng, A. Nanayakkara, M. Challacombe, P.M.W. Gill, B. Johnson, W. Chen, M.W. Wong, C. Gonzalez, J.A. Pople, Gaussian 03, Revision D.01, Gaussian, Inc, Wallingford CT (2004).

[37] N.M. Ruvalcaba, G. Cuevas, I. Gonzalez, M.A. Martinezy, Relationship between Molecular Structure and Electron Targets in the Electroreduction of Benzocarbazolediones and Anilinenaphthoquinones. Experimental and Theoretical Study, J. Org. Chem. 67 (2002) 3673–3681.

[38] A. Satheshkumar, E.H. El-Mossalamy , R. Manivannan , C. Parthiban , L.M. Al-Harbi, S. Kosa, K.P. Elango, Anion induced azo-hydrazone tautomerism for the selective colorimetric sensing of fluoride ion, Spectrochim. Acta, Part A 128 (2014) 798–805.

Figure Captions

Fig. 1 Colour changes observed in aqueous HEPES buffer: DMF (2:8 v/v) solution of **R1** ($5x10^{-4}$ M) upon addition of one equivalent of various anions.

Fig. 2 UV-Vis absorption changes of **R1** [$5x10^{-4}$ M] in presence of various anions

Fig. 3 UV-Vis spectra of **R1** ($5x10^{-4}$ M) with incremental addition of cyanide (0-$5x10^{-3}$ M) in aqueous HEPES buffer: DMF (2:8 v/v) medium

Fig. 4 Fluorescence spectra of **R1** ($5x10^{-4}$ M) with incremental addition of cyanide (0-$5x10^{-3}$ M) in aqueous HEPES buffer: DMF (2:8 v/v) medium

Fig. 5 ^{1}H NMR spectrum of **R1** with addition of (a) 0 equiv. (b) 0.25 equiv. (c) 0.5 equiv. (d) 1 equiv. of cyanide in DMSO-d_6

Fig. 6 ORTEP view and atom numbering for **R3** (Top) and **R4** (Bottom)

Fig. 7 Changes in redox properties of **R1** upon addition of cyanide in DMF

Fig. 8 HOMO-LUMO energy level diagrams for the receptor **R** and **R+CN**$^{-}$

Fig. 9 Colour changes of test strips upon dipping in cyanide ion solution in water

Fig. 1

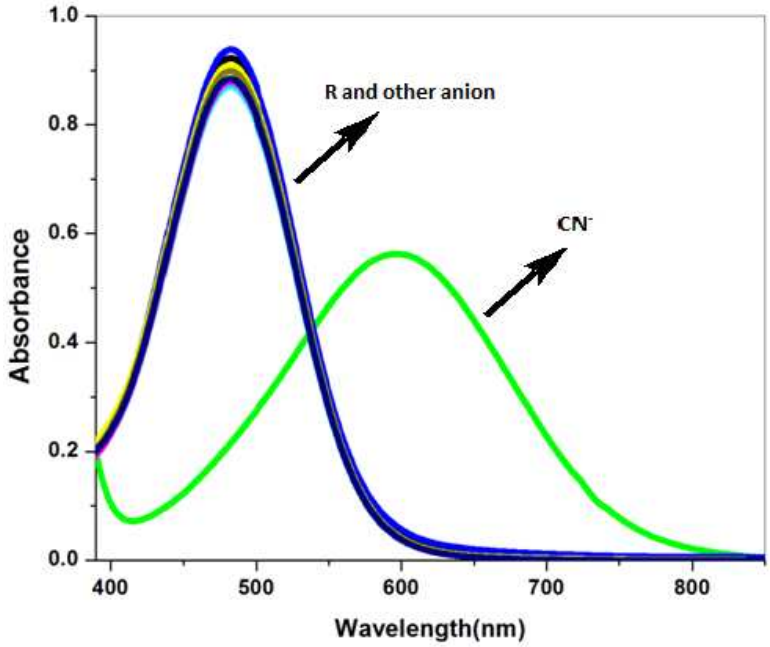

Fig. 2

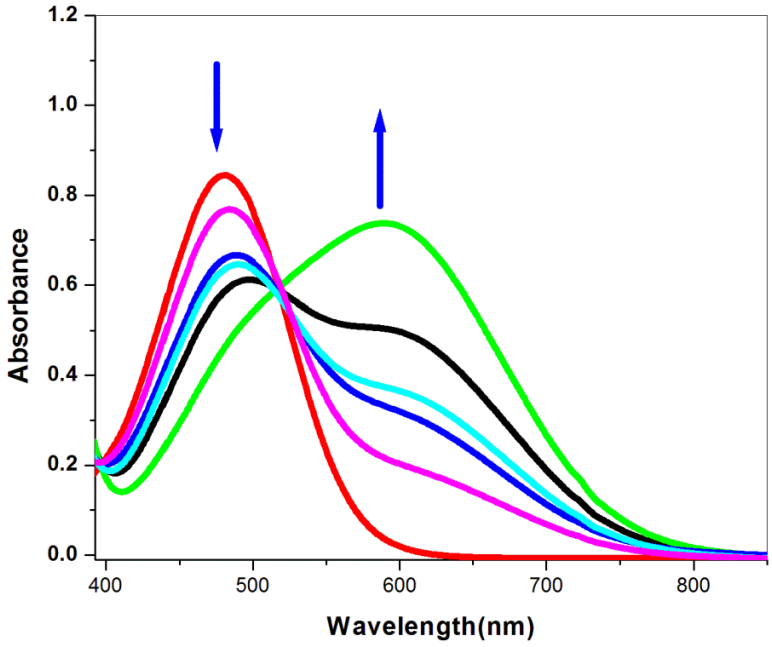

Fig. 3

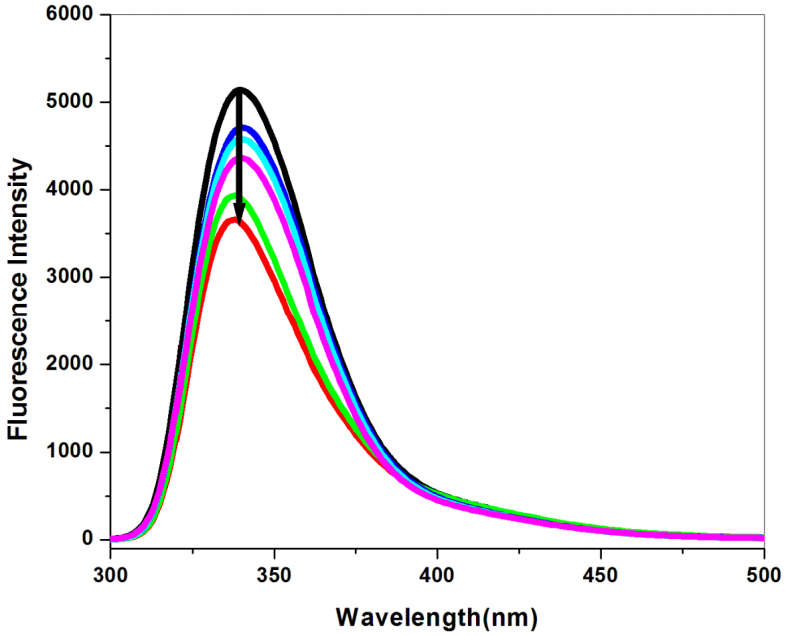

Fig. 4

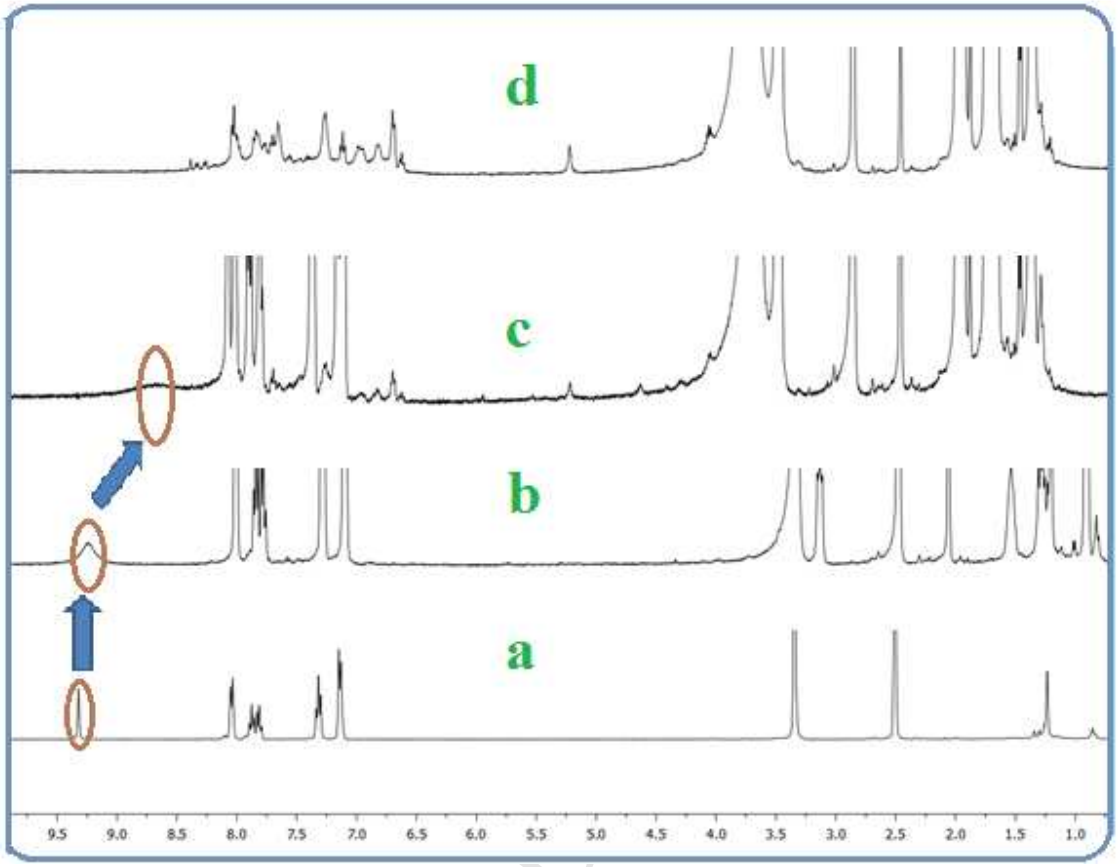

Fig. 5

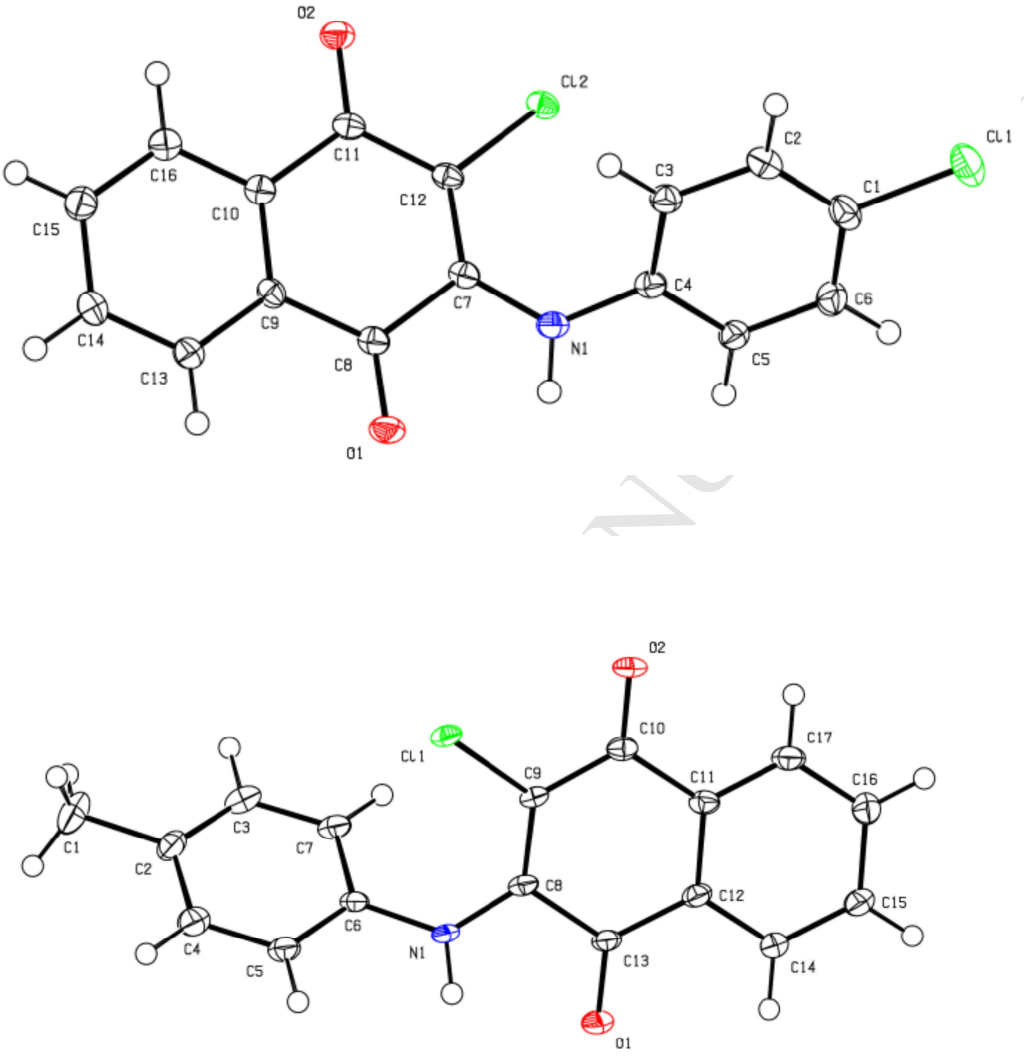
O2
CL2
C11
C16
C10
C12
C15
C7
C9
C14
C8
C13
O1
N1
C4
C3
C2
CL1
C1
C6
C5
O2
C10
C17
CL1
C9
C11
C16
C1
C3
C7
C2
C8
C12
C15
C6
N1
C4
C13
C14
C5
O1

Fig. 6

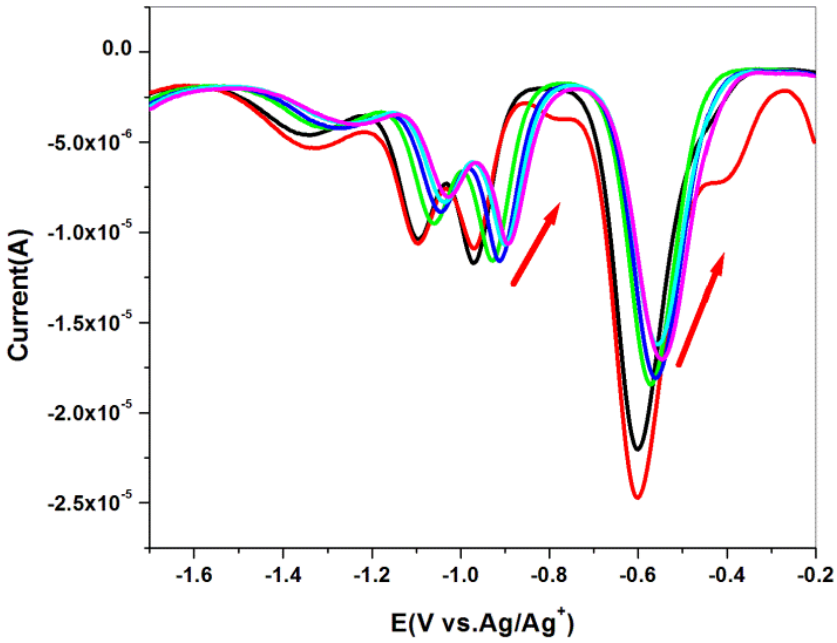

Fig. 7

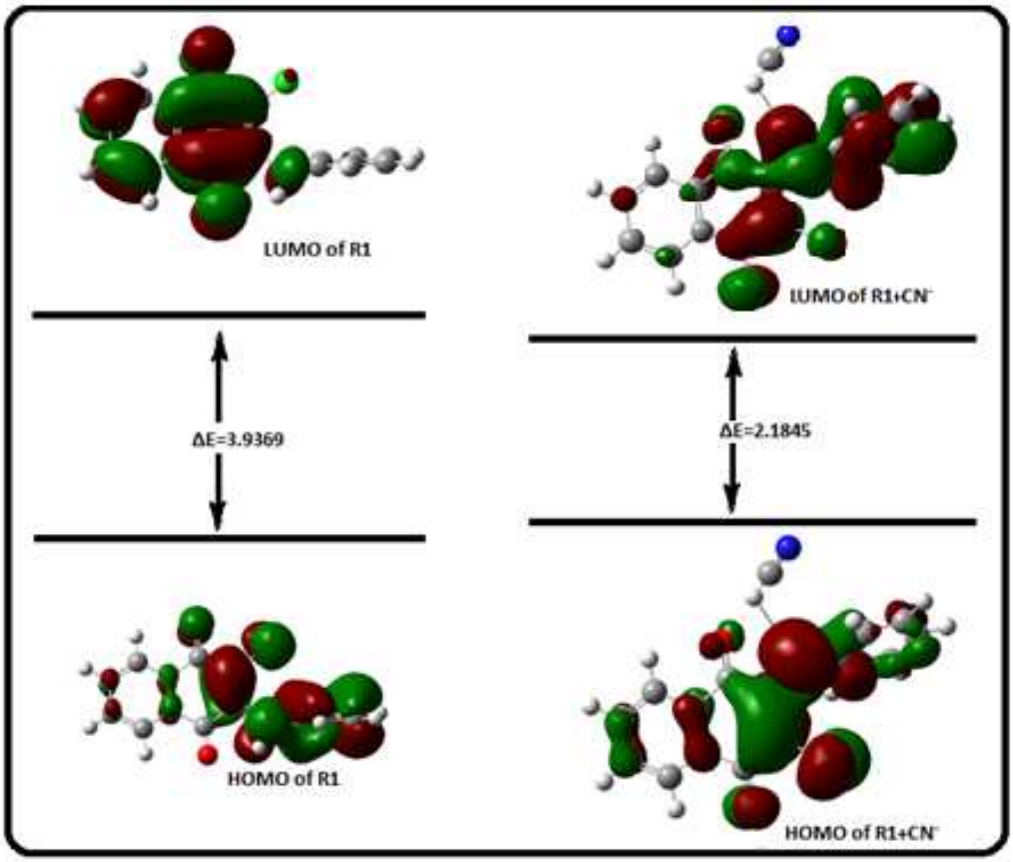
LUMO of R1
ΔE=3.9369
HOMO of R1
LUMO of R1+CN-
ΔE=2.1845
HOMO of R1+CN-

Fig. 8

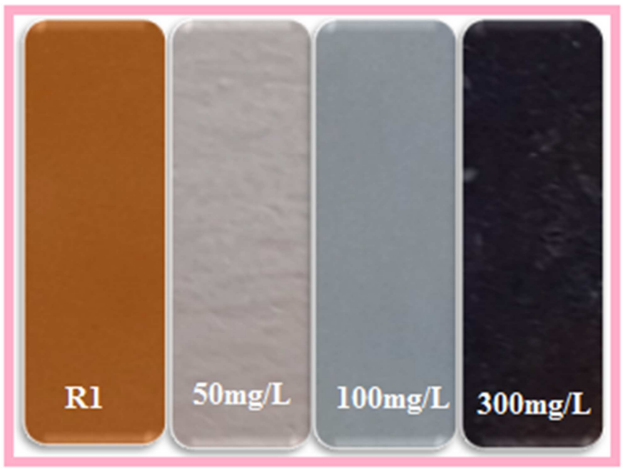

Fig. 9

Table 1. Data obtained from UV-Vis and fluorescence spectra for **R1-R5** in aqueous HEPES buffer: DMF (2:8 v/v) medium

Receptor	λ_{max} (nm)		Red shift	Isosbestic	log ε	Binding	DL*
	R	**R+CN$^-$**	(Δλ nm)	point (nm)		constant (M^{-1})	
R1	481	589	109	517	3.23	$1.6x10^4$	4.5
R2	479	597	118	506	3.03	$4.6x10^4$	0.6
R3	478	594	116	517	3.26	$2.1x10^4$	0.1
R4	488	590	102	531	3.29	$2.5x10^3$	3.5
R5	488	593	105	524	3.30	$1.2x10^3$	3.5

*DL: Detection limit (x 10^{-8} M)

Highlights

- Arylamino-naphthoquinones selectively sense cyanide in aq.solution colorimetrically.
- The mechanism of sensing involves deprotonation.
- Sensing is enabled by substituent dependent resonance effect.
- XRD data confirms the resonance assistance in H-bonding.